Electronic Supplementary Material (ESI) for Journal of Materials Chemistry A.

Supporting Information:

In-situ analysis of the oxygen evolution reaction on the CuO film in alkaline solution by surface interrogation scanning electrochemical microscopy: investigating active sites (Cu^{III}) and kinetics

Seokjun Han, Jinoh Yoo, and Won Tae Choi*

Department of Chemical Engineering, University of Florida, Gainesville, FL 32611, United States

Table of Contents

1. Experimental

1.1. Instrumentation

Experiments for electrodeposition were carried out using a CHI769C potentiostat and SECM experiments were conducted with a CHI920C SECM station and its built-in software (CH Instruments; Austin, TX). The detail of the setup was described in previous literature.[1, 2] The tip was vertically aligned on the substrate at a distance of ca. 2.0μm, where the generation-collection efficiency was unity. Chronoamperometry was chosen as a detection technique in the SI-SECM titration experiments. For each titration, the substrate was pulsed to a potential for 15s, followed by a potential step back to open circuit with the collection on the tip for 15s. The redox mediator solutions employed in the experiments consisted of 1mM ferrocenemethanol in 0.1M KCl for the approach and 1mM ferricyanide in 0.1M KOH for the titration. 1mM ferricyanide were scanned from 300nm to 600nm using spectrophotometry (UV-2600, Shimadzu, Japan) for stability.

1.2. SI-SECM tip-substrate alignment and approach

In a typical SECM cell, two ultramicroelectrode (UME) electrodes are positioned vertically, with the substrate UME pointing upward and the tip UME pointing downward. The substrate UME remains fixed in position with tilt correction through a three-point stage positioner. The motion of tip electrode was governed by stepping motors and piezo controllers operating in the spatial directions of X, Y, and Z. The working electrodes 1 and 2 were linked to the tip and substrate UMEs with a reference electrode of Ag/AgCl (3M KCl) and a counter electrode of platinum. First, once the basic set-up was completed, the cell was filled with the analyte solution (1mM ferrocenemethanol in 0.1M KCl). Second, a CV scan was conducted to determine the $I_{t,ss}$ of the tip (Fig. S1). Third, the substrate was located using imaging mode of the SECM from the tip. Subsequently, the tilt of the stage was varied both in X and Y until the similar current profile (Fig. S2). Following this, another imaging mode of SECM was performed to observe whether the current distribution on the surface with ca. 25 μm diameter and a disk shape was proportional (Fig. S3). If the shape

was not disk-like or the current distribution was not proportional, the X and Y were remodulated. Finally, after the tilt correction and tip-substrate alignment were achieved, tip-substrate approach was slowly performed in the negative feedback mode to minimize the impact on the catalyst during the approach (Fig. S4).[3] By the negative feedback approach curve in the Z direction in good agreement with theoretical curve, the tip was placed at a distance of ca. 2.0 μm from the substrate. The theoretical curve was simulated using the COMSOL simulation of the negative feedback mode.[4, 5]

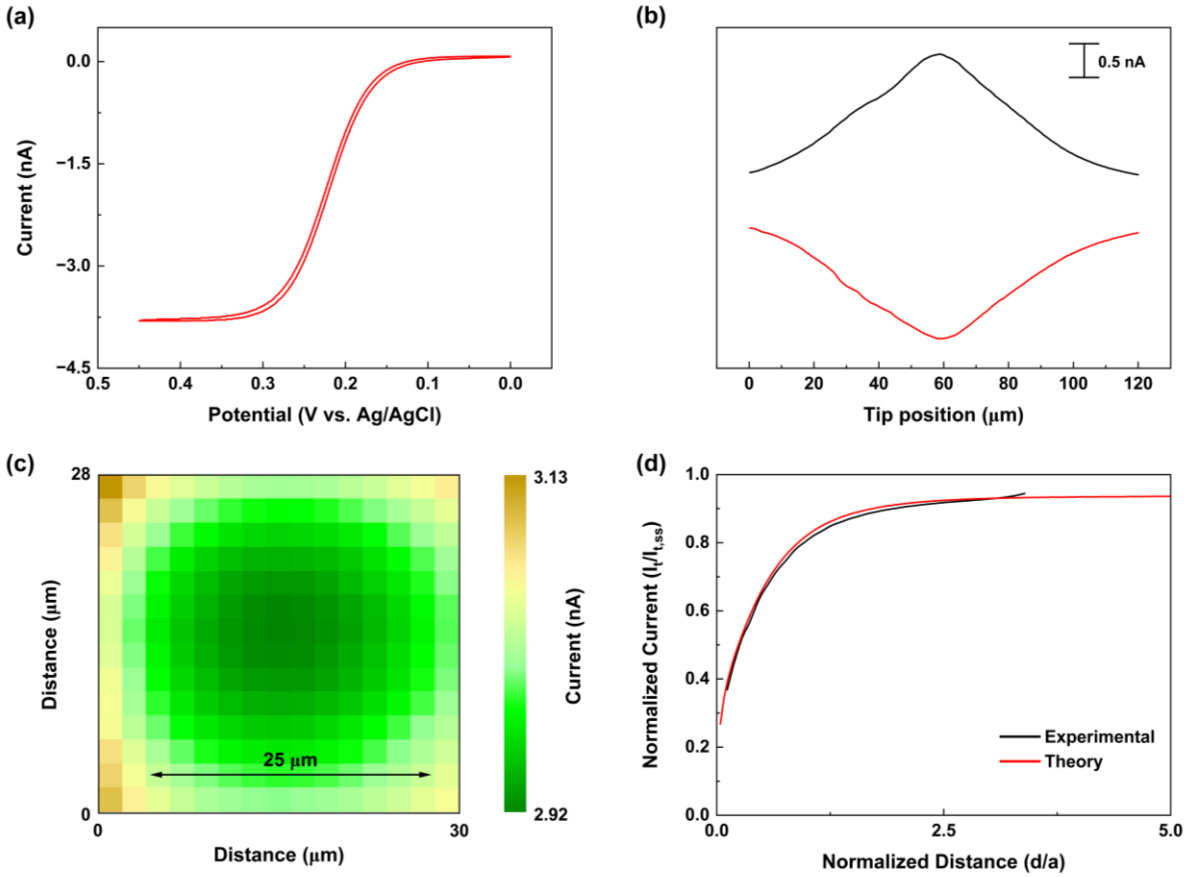

Fig. S1 (a) Cyclic voltammograms of 1mM $FcMeOH^+$ (scan rate, 10 mV s^{-1}). (b) Tip scan in the X and Y direction (Black line: X direction, Red line: Y direction). (c) Image of CuO catalyst on the substrate using SECM mode; Tip potential: 0.45V vs. Ag/AgCl in 1mM $FcMeOH^+$ with 0.1M KCl. (d) Negative feedback approach curve (Black line: Experimental, Red line: Theory) in 1mM $FcMeOH^+$ with 0.1M KCl.

1.3. Steady current of the redox mediator

Two distinct redox mediators were employed: 1mM ferrocenemethanol ($FcMeOH^{+/0}$, $E = 0.22V$ vs. Ag/AgCl) for approach and 1mM ferricyanide ($Fe(CN)_6^{3-/4-}$, $E = 0.20V$ vs. Ag/AgCl) for titration. 1mM ferrocenemethanol, commonly used as a redox mediator for UME, exhibited a steady current at approximately 3.75 nA (Fig. 2a). On the other hand, 1mM ferricyanide demonstrated a steady current at around 4.1 nA (Fig. 2b). The stability of ferricyanide was confirmed in 0.1M KOH through the chronoamperogram and UV-Vis spectroscopy. In the chronoamperogram; from OCP to -0.2 V, the ferricyanide in 0.1M KOH exhibited a stable steady current of 4.1 nA (Fig. 2c). In the UV-Vis spectroscopy, the ferricyanide in 0.1M KOH maintains a stable state at room temperature for extended hours (Fig. 2d).

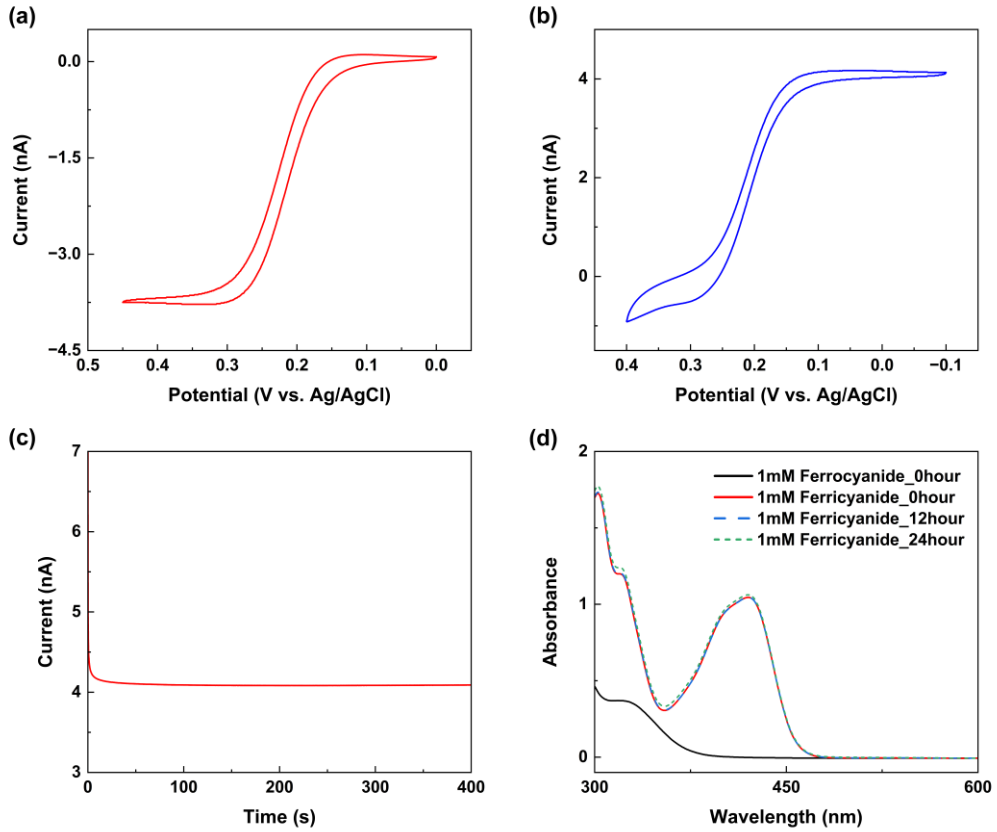

Fig. S2 (a) Cyclic voltammogram of 1mM $FcMeOH^+$ (scan rate, 10 mV s^{-1}). (b) Cyclic voltammogram of 1mM $[Fe(CN)_6]^{3-}$ (scan rate, 50mV s^{-1}). (c) Chonoamperogram of the Au UME in aqueous solution containing 1mM $[Fe(CN)_6]^{3-}$ and 0.1M KOH. (d) UV-Vis adsorption spectrum of 1mM $[Fe(CN)_6]^{3-}$ in 0.1M KOH.

2. Supplementary results and discussion

2.1. Characterizations of CuO

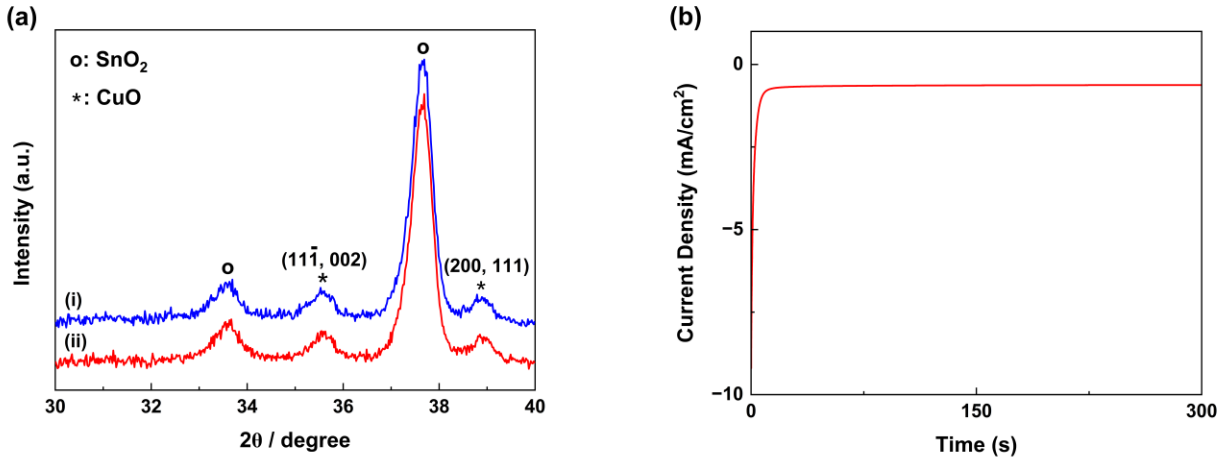

Fig. S3 (a) X-ray diffraction patterns of CuO films on FTO substrate; (i) before and (ii) after the OER. (b) Chronoamperomogram of the CuO/FTO at 0.7 V (vs. Ag/AgCl) for 300s in 0.1M KOH for the OER test.

The CuO film was prepared on fluorine-doped tin oxide (FTO) substrate by galvanostatic polarizations (0.4 mA/cm^2 for 1800s) in 20 mM Cu^{II} tartrate solution. X-ray diffraction (XRD) was conducted to confirm the chemical identity of the CuO structure (**Fig. S3a**), exhibiting lattice constants with a=4.68Å, b=3.43 Å, c= 5.14 Å and a tenorite crystal structure, consisting of four oxygen atoms and four copper atoms in each unit cell.[6, 7] The CuO/FTO was immersed in alkaline solution and potential of 0.7 V (vs. Ag/AgCl) was applied for 300s for the OER (**Fig. S3b**). The chemical nature of CuO was remained the same, confirmed by XRD (**Fig. S3a**).

2.2. Pre-conditioning

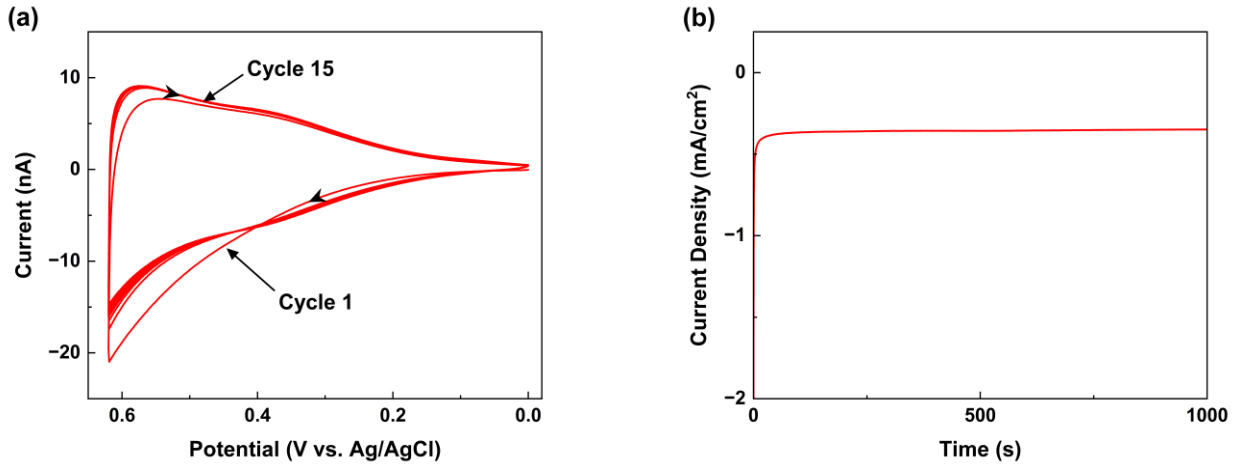

Fig. S4 (a) Cyclic voltammograms of the CuO film for pre-conditioning in 0.1M KOH (scan rate 50 mV s^{-1}) (b) Chronoamperomogram of the CuO film at 0.68 V (vs. Ag/AgCl) in 0.1M KOH.

The CuO film deposited UMEs were immersed in 0.1 M KOH aqueous solution (pH 13) and electrode potential was scanned from 0 to 0.62V (vs. Ag/AgCl) for 15 cycles to remove loosely attached CuO (**Fig. S4a**). The cleaned CuO film showed a stable OER current (**Fig. S4b**).

2.3. Roughness Factor

The CuO deposited on the gold UME was scanned in 0.1M KOH solution using cyclic voltammetry at different scan rates from 10 to 80 mV s^{-1} (**Fig. S5a**). The capacitance of the electric double layer was determined by analyzing the slope of the charging current in relation to the scan rate (**Fig. S5b**).[8] The active surface area of deposited catalyst films can be computed based on the ideal capacitance of a specified area with a flat metal oxide surface.[9] For each experiment, the roughness factor was determined. Therefore, current density, charge density and active site density were calculated based on the roughness factor.

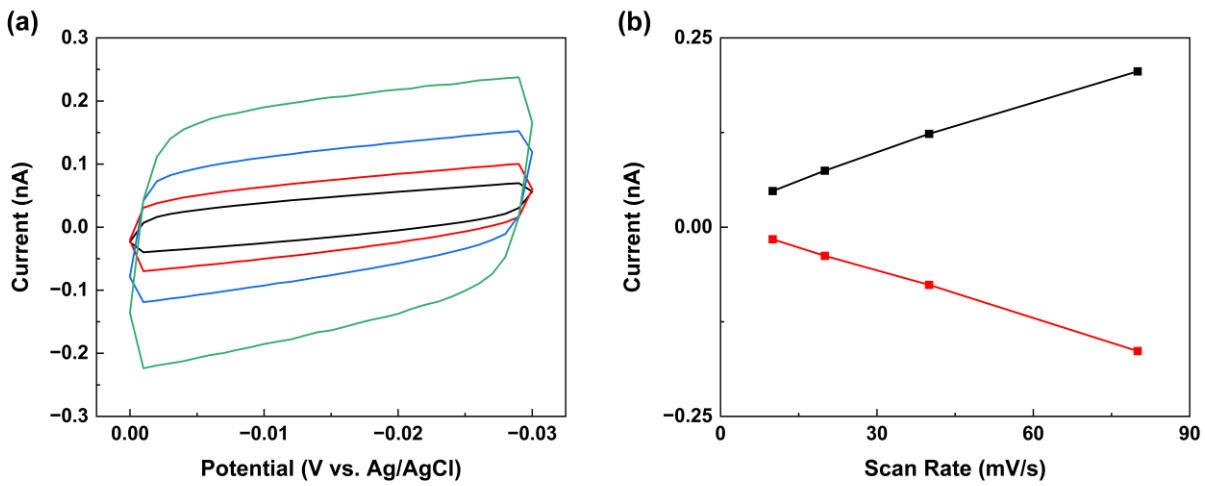

Fig. S5 (a) Cyclic voltammograms of non-Faradaic charging of the CuO catalyst on Au UME at different scan rates; from 10 to 80 mV s^{-1}. (b) Plot of current vs. scan rate for both forward and backward scans.

2.4. The charge density of the titration

Table S1 The charge density of the titration for CuO with roughness factor 7.4

Potential [=] V	Charge [=] C	Charge Density [=] $\mu C/cm^2$
0.30	3.95E-09	108.65
0.40	1.07E-08	293.54
0.50	2.07E-08	569.50
0.60	3.32E-08	912.76
0.64	3.79E-08	1044.66
0.68	4.10E-08	1128.90
0.72	4.437E-08	1203.78
0.74	4.41E-08	1214.79
0.76	4.46E-08	1228.01

Table S2 The charge density of the titration for CuO with roughness factor 8.9

Potential [=] V	Charge [=] C	Charge Density [=] $\mu C/cm^2$
0.30	3.07E-09	70.37
0.40	1.01E-08	230.24
0.50	2.14E-08	489.25
0.60	3.90E-08	892.11
0.64	4.77E-08	1092.87
0.68	5.46E-08	1249.30
0.72	5.87E-08	1344.67
0.74	5.86E-08	1340.53

Table S3 The charge density of the titration for CuO with roughness factor 6.6

Potential [=] V	Charge [=] C	Charge Density [=] $\mu C/cm^2$
0.30	6.19E-09	191.06
0.40	1.36E-08	418.85
0.50	2.20E-08	679.98
0.60	3.25E-08	1003.15
0.65	3.64E-08	1123.53
0.68	3.79E-08	1169.83
0.70	3.91E-08	1206.87
0.72	3.97E-08	1225.39
0.74	4.01E-08	1237.74

Table S4 The charge density of the titration for CuO with roughness factor 7.1

Potential [=] V	Charge [=] C	Charge Density [=] $\mu C/cm^2$
0.30	5.25E-09	150.63
0.40	1.19E-08	341.16
0.50	2.15E-08	618.04
0.60	3.40E-08	975.55
0.64	3.86E-08	1107.25
0.68	4.20E-08	1206.24
0.73	4.50E-08	1290.31
0.74	4.51E-08	1294.04
0.76	4.55E-08	1305.23
0.80	4.53E-08	1299.78

Table S5 The charge density of the titration for CuO with roughness factor 9.0

Potential [=] V	Charge [=] C	Charge Density [=] $\mu C/cm^2$
0.30	7.03E-09	145.50
0.40	1.62E-08	335.92
0.50	2.91E-08	603.13
0.60	4.73E-08	979.00
0.64	5.55E-08	1148.72
0.65	5.64E-08	1167.35
0.68	6.10E-08	1262.56
0.70	6.30E-08	1303.54
0.71	6.40 E-08	1323.61
0.72	6.57 E-08	1359.63
0.73	6.57 E-08	1359.83

2.5. The active site density by the titration

The atomic density of copper on CuO surface can be estimated from the lattice constants and crystal structure. Each unit cell contains 4 oxygen atoms and 4 copper elements with tenorite structure and a lattice constant represented as a=4.68Å, b=3.43 Å, c=5.14 Å. The copper density was about 25 Cu atoms/nm^2 on the CuO surface form eq (S1).

$$4\ \text{Cu atoms} \times \frac{1}{(4.68\times3.43)\ \text{Å}^2} \times \frac{\text{Å}^2}{10^{-2}\ nm^2} \approx 25\ \text{Cu atoms/nm}^2 \quad \text{(S1)}$$

Active site density (Cu^{III} atoms/nm^2) was calculated from charge density ($\mu C/cm^2$) through **eqn (S2)**, where n is the number of electrons for titration.

$$\frac{\mu C}{cm^2} \times \frac{10^{-6}}{\mu} \times \frac{(6.241\times10^{18})\ e^-}{C} \times \frac{1\ cm^2}{10^{14}\ nm^2} \times \frac{1}{n} \quad \text{(S2)}$$

Table S6 Active site density on CuO surface

Set	Roughness Factor	Charge Density [=] $\mu C/cm^2$	Active site density if step 3 is RDS	Active site density if step 4 is RDS
Set 1	7.4	1228.01	25.5	19.1
Set 2	8.9	1340.53	27.9	20.9
Set 3	6.6	1237.74	25.7	19.3
Set 4	7.1	1299.78	27.0	20.3
Set 5	9.0	1359.83	28.2	21.2

2.6. Mechanism analysis for CuO

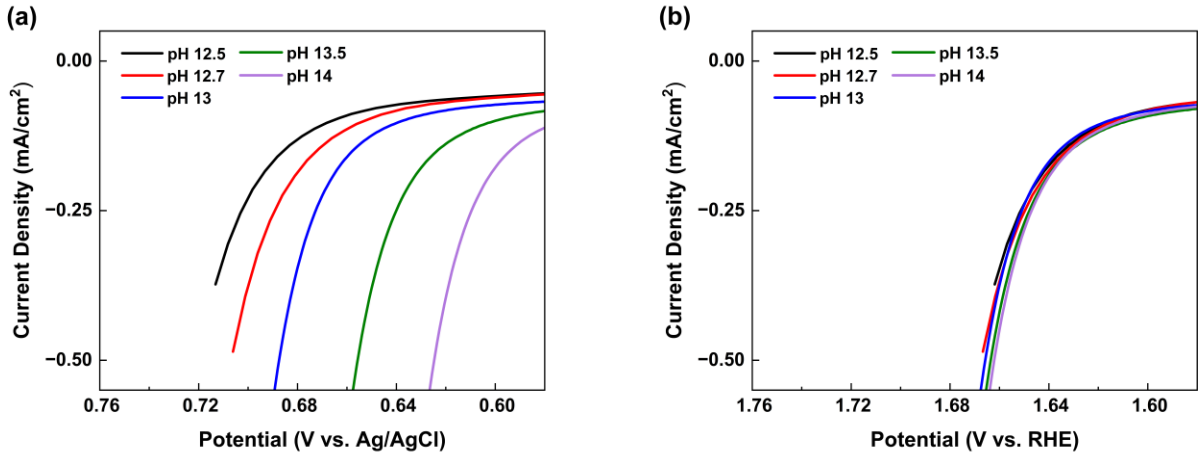

Fig. S6 pH dependence of the OER activities of CuO (scan rate, 10mV s^{-1}) (a) Scale of Ag/AgCl reference. (b) Scale of RHE.

If the catalyst has low OH′coverage, the **eqn (6)** can be regarded as the pre-equilibrium and can be represented as **eqn (S4)** using the Nernst **eqn (S3)** with the water's activity considered as 1.

$$u = u^o - \frac{RT}{nF} \ln \Pi a_i^{s_i} \tag{S3}$$

$$u = u^o - \frac{RT}{F} \ln \frac{\alpha_{OH'}}{\alpha_{OH^-}} = u^o - \frac{RT}{F} \ln \frac{C_{OH'}}{C_{OH^-}} \tag{S4}$$

Through **eqn (S4)**, $C_{OH'}$ term is expressed by **eqn (S9)**.

$$u = u^o + 2.303 \frac{RT}{F} (pOH) + \frac{RT}{F} \ln (C_{OH'}) \tag{S5}$$

$$u = u^o + 2.303 \frac{RT}{F} (pK_w - pOH) + \frac{RT}{F} \ln (C_{OH'}) \tag{S6}$$

$$u - u^o + 2.303 \frac{RT}{F} (pH) = \frac{RT}{F} \ln (C_{OH'}) \tag{S7}$$

$$u - u^o_{eff} = \eta = \frac{RT}{F} \ln (C_{OH'}) \tag{S8}$$

$$C_{OH'} = e^{f\eta} \tag{S9}$$

2.7. Measurement of the pseudo-first-order rate

A simple case is shown below considering step 3 is rate-determining step (RDS).

$$Cu^{III}\text{-}OOH + OH^- \rightarrow Cu^{II} + O_2 + H_2O \quad \text{(S10)}$$

Equation of converting charge density ($\mu C/cm^2$) into surface concentration (mol/m^2)

$$\frac{\mu C}{cm^2} \times \frac{10^{-6}}{\mu} \times \frac{1\ mol}{9.65\times10^4\ C} \times \frac{100^2\ cm^2}{m^2} \quad \text{(S11)}$$

Equation of pseudo-first-order rate constant

$$\frac{d[Intermediates]}{dt} = -k'[Intermediates] \quad \text{(S12)}$$

$$\ln[Intermediates] = -k't + Constant \quad \text{(S13)}$$

Table S7 Pseudo-first-order reaction rate constant

Set	Tip-substrate distance [=] μm	Rate Constant at mid $C_{OH'}$ coverage	Rate Constant at high $C_{OH'}$ coverage
Set 1	2.0	0.0237 (0.65 V)	0.0233 (0.73V)
Set 2	1.9	0.0175 (0.65V)	0.0173 (0.73V)
Set 3	2.7	0.0177 (0.65V)	0.0175 (0.70V)
Set 4	2.4	0.0148 (0.65V)	0.0151 (0.75V)
Set 5	1.9	-	-

3. References

1. H. S. Ahn and A. J. Bard, *Analytical chemistry*, 2015, **87**, 12276-12280.
2. J. Rodríguez-López, M. A. Alpuche-Avilés and A. J. Bard, *Journal of the American Chemical Society*, 2008, **130**, 16985-16995.
3. H. S. Ahn and A. J. Bard, *The Journal of Physical Chemistry Letters*, 2016, **7**, 2748-2752.
4. J. Kwak and A. J. Bard, *Analytical Chemistry*, 1989, **61**, 1221-1227.
5. R. Cornut and C. Lefrou, *Journal of Electroanalytical Chemistry*, 2007, **604**, 91-100.
6. M. Izaki, T. Koyama, P. L. Khoo and T. Shinagawa, *ACS omega*, 2019, **5**, 683-691.
7. P. Poizot, C.-J. Hung, M. P. Nikiforov, E. W. Bohannan and J. A. Switzer, *Electrochemical and Solid-State Letters*, 2002, **6**, C21.
8. D. Voiry, M. Chhowalla, Y. Gogotsi, N. A. Kotov, Y. Li, R. M. Penner, R. E. Schaak and P. S. Weiss, *Journal*, 2018, **12**, 9635-9638.
9. S. Levine and A. Smith, *Discussions of the Faraday Society*, 1971, **52**, 290-301.